

# Thermo Mechanical and Metallurgical Phenomena of FSW of Al-steel, Al-Ti

Shubhavardhan R N

Department of Mechanical & Industrial Engineering  
Ryerson University, Toronto, Canada

**Abstract**— Friction stir welding (FSW) is a solid-state joining technique which can be used for joining not only traditionally weldable aluminum alloys but also high strength aluminum and other metallic alloys that are hard to weld using conventional fusion welding processes. Mechanical strength of FSL welds under static loading is commonly determined using tensile shear testing and fracture strength ( $\sigma_{Lap}$ ) corresponding to the maximum load in a test over the sample width is widely used the strength value. In (friction stir lap welding) FSLW of dissimilar metallic alloys with large differences in melting temperatures, a metallurgical bond is established through the formation of interfacial intermetallics. However, as these intermetallic compounds are generally believed to be brittle with limited ductility, they are commonly viewed to adversely affect  $\sigma_{Lap}$ . The aim of the present research is to study how the interface structure is affected by FS conditions and how the formation of interface structure affects  $\sigma_{Lap}$  of Al-Steel and Al-Ti FSL welds.

**Keywords**—Friction stir lap welding, aluminum, steel, titanium, intermetallics, fracture strength.

## I. INTRODUCTION

Friction stir lap welding of dissimilar alloys such as Al-to-steel, Al-to-Ti or Al-to-Cu is also of enormous significance in many industries. In this paper, we focus on an example of FSLW of one metallic alloy to another with considerably higher melting temperature - FSLW of Al-steel and Al-Ti. It is well known that fusion welding of Al-to-steel and Al-Ti is very challenging [1, 2]. In FS welding of Al-steel and Al-Ti, aided by frictional and deformation heat, metallurgical bond is established through diffusion and subsequent formation of interfacial intermetallic, as indicated in Fig. 1 for FSLW. It is clear that a metallurgical bond is a condition for a quality joint, although intermetallics are commonly viewed to affect joint strength adversely [3-4]. There have been a number of studies on FSLW of Al-Steel [5, 6, 7-10]. Early investigation by Elrefaey et al [6] on Al/Steel FSLW clearly established that the tool pin slightly (~0.1 mm) penetrating to steel is a condition for a metallurgical joint to be established at the Al-Steel interface, resulting in a good joint strength. Although detailed quantification was not done in their study, it was clear that the interface region of welds made with pin penetration is a highly irregular structure of mix layers. Coelho et al. [5] names the irregular interface region as mixed stir zone. The thin layers, significantly less than 0.5  $\mu\text{m}$  in thickness are

laminated with recrystallized fine grains of  $\alpha$ -Fe in this mixed stir zone. Kimapong et al [20, 9] was an attempt to correlate the  $\sigma_{Lap}$  to the thickness of the intermetallic layer, under the condition of pin penetration. Their data shows that in general increasing intermetallic compound thickness reduces  $\sigma_{Lap}$ , however the meaning of the referred intermetallic thickness is unclear and misleading. In most studies on FSLW of Al-Steel, tensile shear testing has been used for evaluating the joint strength. Kimapong et al [9] reported  $\sigma_{Lap}$  values, ranging from 280 N/mm to 559 N/mm for a wide range of FSLW and pin penetrating conditions. However the reason is unclear as to why some of their welds displaying severe discontinuity with voids along the interface region, exhibited high values.

Al-Ti FSLW was conducted by Chen and Nakata [11]. Many void defects formed at the side of titanium because of insufficient flow behavior of titanium during FSLW. However when the pin did not penetrate the titanium plate, the joint exhibited high  $\sigma_{Lap}$  value of 469 N/mm. they also suggested that AlTi<sub>3</sub> intermetallic phase formed at the interface region, based on x-ray diffraction patterns obtained from the fracture surfaces of tested samples. However their results may not be accurate as no visible intermetallic layer can be seen in SEM micrograph of interface region. Chen et al [12] conducted detailed quantification was not completed in their study, it can be seen from their micrographs that the interface region of welds is a highly irregular structure of mix layers. Review of literature on other solid-state joining techniques such as diffusion bonding [13] and friction welding [13-17] shows that TiAl<sub>3</sub> intermetallic layer formed at the Al-Ti interfaces. However the intermetallic layer has been reported to be very thin (less than one micron) due to insufficient thermal energy for intermetallics growth. On the other hand, formation of several micron thick TiAl<sub>3</sub> intermetallic layers has been commonly observed in fusion welding of Al-Ti welds [18, 19]. That is because fusion welding techniques are all conducted at temperatures above the melting point of aluminum, and thus higher peak temperature of welding together with presence of liquid aluminum enhance the diffusion rate of Al-Ti atoms and thus faster growth of intermetallic layer. Therefore formation of TiAl<sub>3</sub> phase at the Al-Ti interface is widely recognized to provide metallurgical bonding in Al-Ti joints. In this paper FSLW of Al-to-steel and Al-Ti, to explain how interface microstructures affect the fracturing process during tensile-shear testing and thus joint strength. A possible control method for producing Al-to-steel and Al-Ti welds for a higher joint strength can then be suggested.

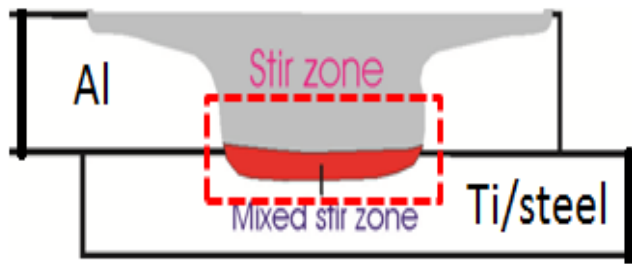


Fig.1. Schematic Illustration of interfacial intermetallics in mixed stir zone

**II. EXPERIMENTAL PROCEDURE**

All FSLW experiments were conducted using a milling machine and thus the mode of FS was displacement control. Schematic illustration of FSLW process has been provided in Fig. 2 shows an actual FSLW experiment. A Lowstir™ device, which is also shown in Fig. 2, was used in each FSLW experiment to monitor the downforce ( $F_z$ ). This monitoring was necessary when a very precise positioning was needed for the case of Al-to-steel welding. Monitoring of temperature in the joining location was also conducted, by placing 0.2 mm K-type thermocouple wires in the lapping location to be FSL welded.

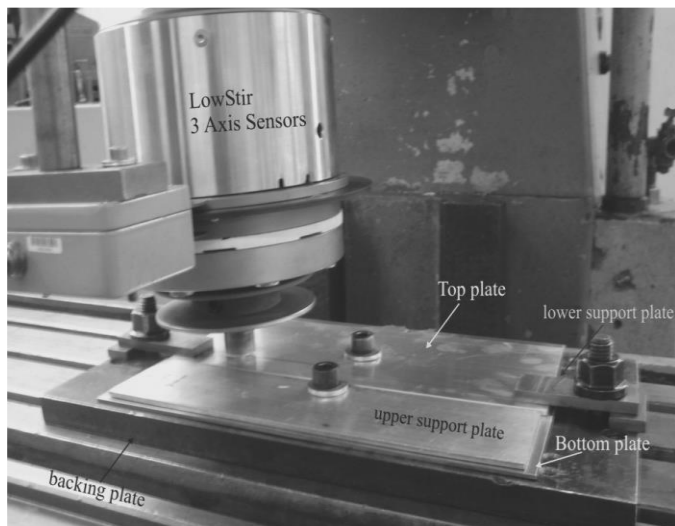


Fig.2. FSLW using a milling machine with a Lowstir™ force measuring device

Work piece materials were A6060-T5 aluminum alloy plates 6 mm thick, Titanium and mild steel of 2 mm thick. Both top and bottom plates were 200 mm long and 100 mm wide. Tools were made using H13 tool steel and the left-hand threads of the pins were made with a 1 mm pitch and a 0.6 mm actual depth. The diameter of the concave shoulder was 20 mm for Al-to-steel/Ti FSLW and the pin outside diameter was 6 mm. A tool tilt angle ( $\Theta$ ) of  $2.5^\circ$  was used. In the present experiments,  $v$  ranged from 20 to 630 mm/min and  $\omega$  ranged from 500 to 2000 rpm. For the work reported here, the penetration depth  $D_p$  in Fig. 3 was varied for FSLW of Al-to-steel/Ti.

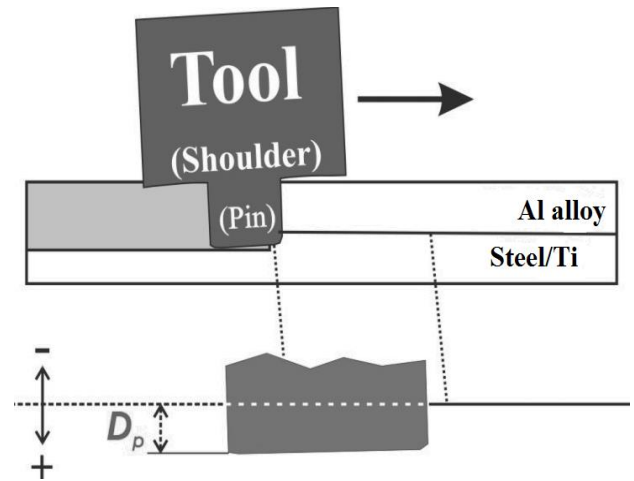


Fig3. Schematic illustration of tool positioning during FSLW showing pin penetration depth

For microstructure observation, the welds were cross-sectioned, mounted and polished following the normal metallographic procedure. Microstructure examination was conducted using a normal optical microscope and a Hitachi SU-70 FE SEM with a Thermo Scientific NSS EDS/EBSD system. Tensile-shear testing of lap welds has been the major method used for evaluating strength of FSL welds in literature. This test method was adopted in this study. Test samples, 16 mm wide, perpendicular to the welding direction were machined from the welded plates. Fig. 4 illustrates the positioning of a sample together with supporting pieces. Samples were tested at a constant crosshead displacement rate of 3 mm/min using a 50 KN Tinius Olsen tensile machine, with a 50 mm extensometer attached. The strength of a lap sample cannot be expressed using the normal load/area, as the stress distribution along the joint area during tensile-shear test is highly uneven. Instead, maximum failure load in a test divided by the width of the sample,  $F_m/w_s$ , is taken as strength.

**III. RESULTS AND DISCUSSIONS**

*A. Al-Steel Microstructure & fracture strength:*

Only two selected samples are shown here to illustrate the importance of interface microstructures and based on this illustration a suggestion of FSLW control for maximum strength can then be made. Fig.4 is the first example and a mixed stir zone (MSZ) commonly observed [20-22] is shown between the top Al plate and the bottom steel plate. The area of MSZ largely corresponds to the area of the pin penetrated into steel (in a 2D cross section) and this zone is a mixture of Fe-Al intermetallic thin pieces embedded in the recrystallized  $\alpha$ -Fe grains.



Fig.4. Cross sectional view of an Al-to-steel weld made with  $\omega = 1,400$  rpm,  $v = 20$  mm/min and  $D_p \approx 0.3$  mm displaying MSZ

With a MSZ, a metallurgical bond between Al and steel is established and thus a slight pin penetration (a slight positive  $D_p$  value, referring to Fig. 3) is commonly believed to be the condition for a good weld strength [20-22]. Naturally, a MSZ cannot form and if  $D_p \ll 0$ . However, FS tool can be position controlled so that  $D_p \approx 0$ . In this case, although there can still be an absence of MSZ, a thin Fe-Al interface intermetallic layer can form, metallurgically bonding the top and bottom plates together, as demonstrated by an example shown in Fig. 5.

Two examples of tensile-tested curves are shown in Fig. 6 for the two different  $D_p$  conditions. For the penetrated sample, the amount of deformation before final fracture and thus fracture energy are not low. The weld strength at 299 N/mm is significantly higher than that of Mg FSL welds (255 N/mm) but is considerably lower than that of Al FSL welds (> 400 N/mm), for  $h = 0$ .

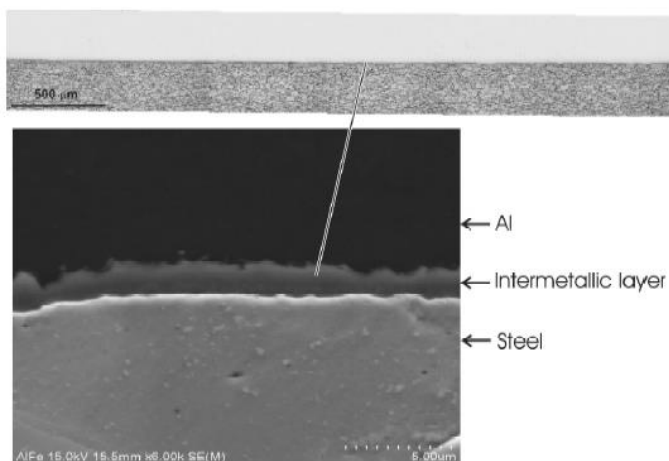


Fig.5. Cross sectional view of an Al-to-steel weld made with  $\omega = 1,400$  rpm,  $v = 20$  mm/min and  $D_p \approx 0$  mm displaying no MSZ but an interface layer

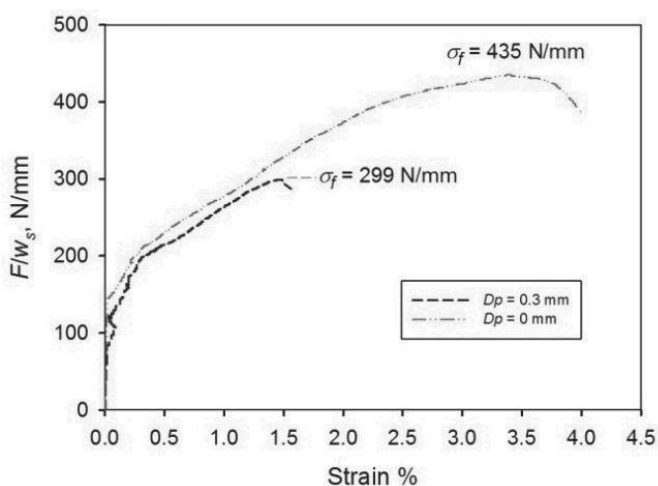


Fig.6. Tensile-shear curves of two samples of welds made with  $\omega = 1,400$  rpm,  $v = 20$  mm/min and  $D_p$  values as indicated

The weld strength at 299 N/mm is close to the values of  $\sim 315$  N/mm which is the maximum value for a large group of

samples using a slight pin penetration [22]. In this latter study, when a weld is free of macro-defects the strength equivalent value is close to that maximum value, regardless of what the FS speed condition was. In order to understand this, an analysis was conducted on a specially tested sample in the present work. As is clearly shown in Fig. 7, cracks propagated in MSZ, likely along the more brittle Fe-Al intermetallic pieces and occasionally stopped by the tougher  $\alpha$ -Fe grains. If this is the common fracture feature and the required fracture strength will then be similar once a MSZ is established, regardless of what the FS condition is so long as the weld is free of macro-defects.

When  $D_p \approx 0$  and an interface layer is established without MSZ, as shown in Fig.6, fracture strength (435 N/mm) is considerably higher than that for the sample with MSZ (299 N/mm). The amounts of deformation and fracture energy as indicated by the curve suggest a considerably tougher weld made by the zero  $D_p$  condition. These are clear by viewing the tested samples in Fig.8. For the pin penetrated sample ( $D_p \approx 0.3$  mm), the sample having been slightly bent is evident. On the other hand, for the zero  $D_p$  sample, a large amount of local deformation and bending before the final fracture is clearly the feature. The absence of MSZ in the zero  $D_p$  sample means a different fracture behavior. The large amounts of deformation and fracture energy for this sample means that the thin interface layer is not brittle under tensile-shear condition. From the present results, it can be suggested that careful positioning control for Al-to-steel FSL welds is a mean for the optimal weld strength to be obtained.

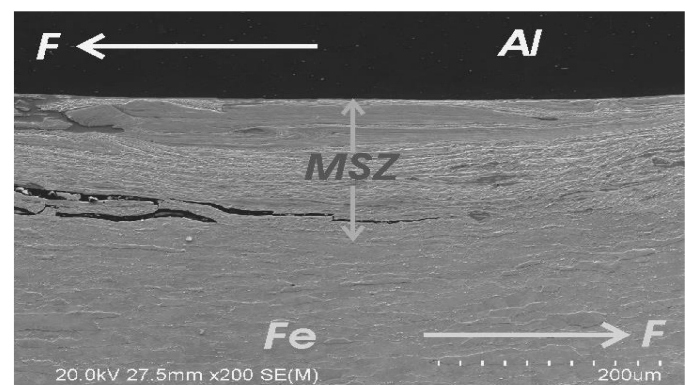


Fig.7. SEM micrograph taken in MSZ region of a weld made with  $\omega = 1,400$  rpm,  $v = 20$  mm/min and  $D_p \approx 0.3$  mm and tested to 270 N/mm ( $\sim 90 F_m/w_s$ )

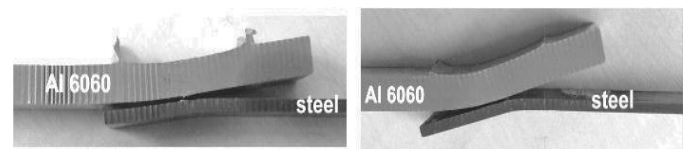


Fig.8. Tensile-shear tested samples of welds made with  $\omega = 1,400$  rpm,  $v = 20$  mm/min and (a)  $D_p \approx 0.3$  mm and (b)  $D_p \approx 0$  mm

Selected fractographs of tested samples are presented in Fig 9. The cracks seen in Fig 9a must be thin as the thickness of the

intermetallic layer and normal to the shear direction, thus contributing little to the shearing process resulting in ductile fracture. A significant portion of the fracture surface as shown in Fig 9b displayed brittle fracture feature. It is likely that cracking propagated along (parallel to) the thin intermetallic layers in the penetrated laminate region during testing.

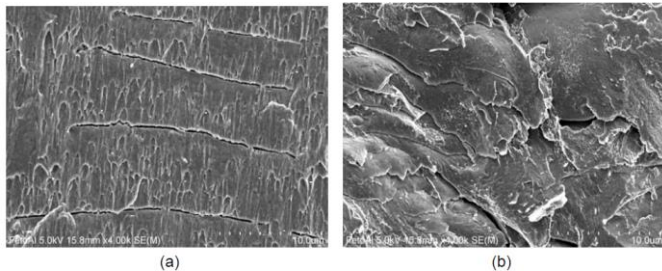


Fig.9. Fracture surfaces of the tensile-shear tested samples (a) ductile and (b) brittle fracture

**B. Al-Ti microstructure and fracture strength:**

Microstructure corresponding to the sample 1 with  $D_p \approx 0$  pin penetration is shown in Fig.10a with low magnification SEM micrograph, however a very thin continuous intermetallic layer (with average thickness of approximately  $\sim 200$  nm) can be seen in the SEM micrograph of interfacial region Fig 10b. It should be noted that characterization of intermetallic layer was not possible in this study due the very thin thickness of interfacial intermetallic layer. However formation of  $TiAl_3$  intermetallic compound in Al-Ti FSL welds has been reported in literature [21]. High  $\sigma_{Lap}$  value (732 N/mm) obtained for no pin penetration tested sample indicates that this very thin intermetallic layer created a strong continuous metallurgical bond at Al-Ti interface.

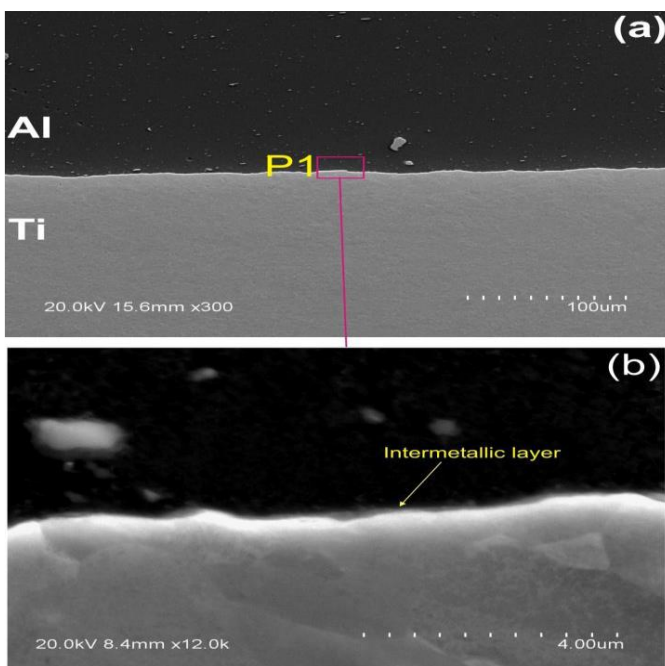


Figure.10 Microstructure of no penetration sample as (a) low magnification SEM micrograph (b) high magnification SEM micrograph showing a very thin interfacial intermetallic layer

For sample 2, significant pin penetration took place ( $D_p \approx 0.3$  mm) as seen in Fig 11. Thus an irregular laminate of titanium and Ti-Al intermetallic layers formed in penetrated region (Fig11b-c), which is similar to the observations made in literature [21], when the pin penetrating condition used. Also a number of micro-cracks formed in the penetrated region (Fig11b-c) which is likely due to strain caused by considerable difference in thermal expansion coefficients of titanium and of aluminum. Furthermore the pin penetration and insufficient material flow of titanium alloy during FSLW resulted in formation of many voids in penetrated region (Fig11d). Presence of micro-cracks and void in the weld, resulted in relatively low  $\sigma_{Lap}$  value (340 N/mm) for the sample 2.

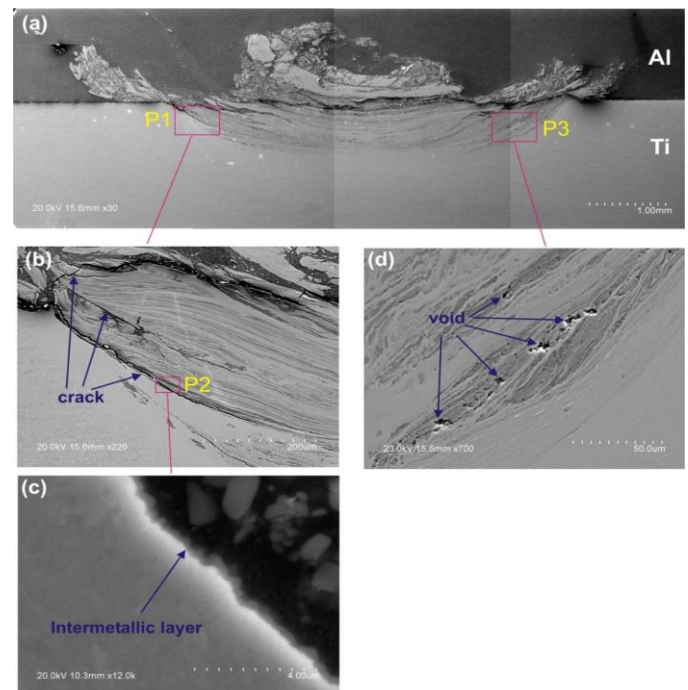


Figure.11 Microstructure of sample 2 (a) macrograph (b) higher magnification micrograph of area P1 in Figure 11a showing the cracks formed in the penetrated region (c) higher magnification micrograph of area P2 in Figure 11b showing intermetallic layers in the penetrated region (d) higher magnification micrograph of area P3 in Figure 11a

During tensile shear testing, sample1 fractured along the Al-Ti interface (Fig 12a) and Al 6060-T5 plate rotated considerably before failure. The bright portion seen on fracture surface of titanium side of tested sample (Fig 12b) indicates that fracture surface is covered by the smeared residue of aluminum. Closer view of fracture surface (Fig 12 c-e) clearly shows that a ductile fracture is dominant with plastic (shear) deformation preceding failure in aluminum adjacent to and on top of the interfacial intermetallic layer. Also EDS map analysis of fracture surface (Fig12 f-g) clearly reveals the presence of smeared aluminum (heavily deformed) on top of fracture surface.

The aluminum macro tear ridge adhered to the fracture surface (Fig12 c-d) indicates the strong cohesion at the interfaces of Ti/intermetallic/Al so that fracture occurred at aluminum side. Moreover, no intermetallic cracking (underneath the smeared

aluminum) can be observed on fracture surface, These results suggest that the interface structure for sample 1 (with a single continuous intermetallic layer) is highly shear fracture resistant and thus high  $\sigma_{Lap}$  value (732 N/mm) obtained during testing.

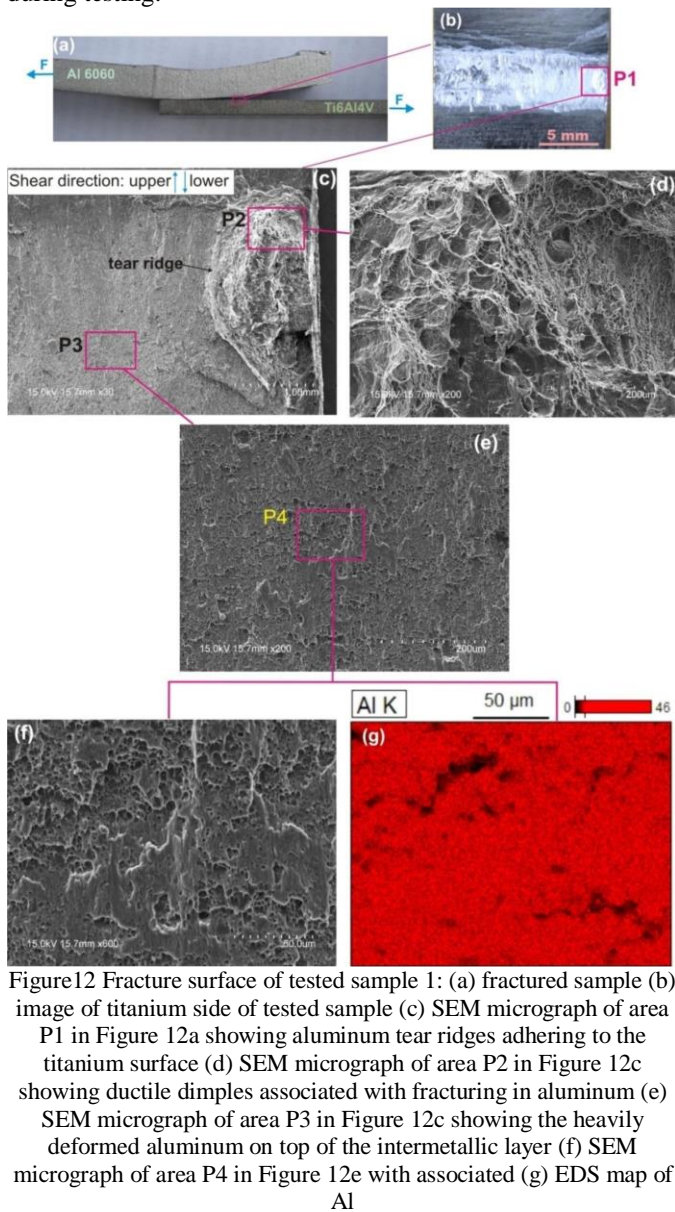


Figure 12 Fracture surface of tested sample 1: (a) fractured sample (b) image of titanium side of tested sample (c) SEM micrograph of area P1 in Figure 12a showing aluminum tear ridges adhering to the titanium surface (d) SEM micrograph of area P2 in Figure 12c showing ductile dimples associated with fracturing in aluminum (e) SEM micrograph of area P3 in Figure 12c showing the heavily deformed aluminum on top of the intermetallic layer (f) SEM micrograph of area P4 in Figure 12e with associated (g) EDS map of Al

Figure 13 shows the sample 2 with  $D_p \approx 0.3$ , tensile shear tested to fracture. The fractographs in Fig 13 c-d clearly shows that significant portion of the fracture surface is of brittle failure. The flake-like features formed on fracture surface suggest that cracking propagated along (parallel to) the intermetallic layers inside the laminate (penetrated) region. Therefore smaller amount of Al 6060-T5 rotation occurred before failure (Fig 13a), compared to tested sample 1 (Fig 12a), indicating smaller plastic deformation during testing.

The fracture surface characteristics of sample 2 are very similar to those observed on fracture surface of Al-Steel weld, when the pin penetrated to steel. These results suggest that the pin penetrating condition in FSLW of either Al-Steel or Al-Ti

results in interface microstructures in which cracking tends to propagate along (parallel to) the irregular intermetallic layers inside the penetrated region. Furthermore microcracks formed in the penetrated region, in FSL welds of either Al-Steel or Al-Ti, can act as favorable cracking initiation source (under loading) and facilitate the fracturing with lower  $\sigma_{lap}$ .

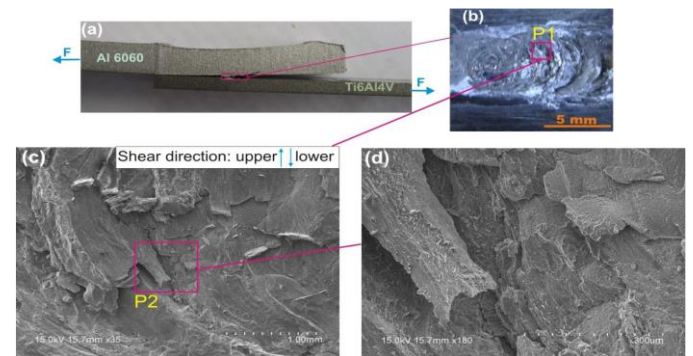


Figure 13 Fracture surface of tested sample 2: (a) fractured sample (b) image of titanium side of tested sample (c) SEM micrograph of area P1 in Fig 13b displaying brittle fracture features (b) higher magnification micrograph of area P2 in Fig 13

#### IV. CONCLUSIONS

For Al-Steel FSL welds, joint strength was found to be very sensitive to pin positioning during FSLW. When the bottom of pin reached the steel surface without penetrating ( $D_p \approx 0$  mm) during FSLW, a single continuous intermetallic layer formed along the interface; and thus continuous metallurgical bonding established. The joint produced by this non pin penetrating condition (with a single continuous intermetallic at interface) displayed a high  $\sigma_{Lap}$  value (435 N/mm) which was  $\sim 42\%$  increase in  $\sigma_{Lap}$  in comparison to the case of pin penetrating condition ( $D_p \approx 0.3$  mm)  $\sigma_{Lap}$  304N/mm (with the mixed interface region). For Al-Ti FSL welds, the pin positioning during FSLW was also found to be the major parameter affecting  $\sigma_{Lap}$  of welds, similar to Al-Steel FSLW. For the sample made using non pin penetrating condition of  $D_p \approx 0$  mm, a thin continuous intermetallic layer formed along the joint interface resulting in a strong metallurgical bonding with high  $\sigma_{Lap}$  value (735 N/mm) during testing. However the pin penetrating condition had detrimental effect on joint strength (435 N/mm) due to formation of voids and micro-cracks in the penetrated region.

#### REFERENCES

[1] E. Taban, J.E. Gould, J.C. Lippold, Dissimilar friction welding of 6061-T6 aluminum and AISI 1018 steel: Properties and microstructural characterization, Materials and Design 31 (2010) 2305-2311.

[2] G. Liedl, R. Bielak, J. Ivanova, N. Enzinger, G. Figner, J. Bruckner, M. Pasic, M. Pudar, S. Hampel, Joining of aluminum and steel in car body manufacturing, Physics Procedia 12 (2011) 150-156.

- [3] A. Elrefaey, M. Gouda, M. Takahashi, K. Ikeuchi, Characterization of aluminum/steel lap joint by friction stir welding, *Journal of Materials Engineering and Performance* 14 (2005) 10-17.
- [4] K. Kimpapong, T. Watanabe, Lap joint of A5083 aluminum alloy and SS400 steel by Friction Stir Welding, *Materials Transactions* 46 (2005) 835-841
- [5] R. S. Coelho, et al., Microstructure and Mechanical Properties of an AA6181-T4 Aluminium Alloy to HC340LA High Strength Steel Friction Stir Overlap Weld. *Advanced Engineering Materials*, 2008. **10**(10): p. 961–972.
- [6] A. Elrefaey, M. Gouda, and M. Takahashi, Characterization of aluminum-steel lap joint by friction stir welding *Journal of Materials Engineering and Performance* 2005. **14**(1): p. 10-17.
- [7]. Y. C. Chen and K. Nakata, Effect of surface state of steel on the microstructure and mechanical properties of dissimilar metal lap joints of aluminium and steel by friction stir welding. *Metallurgical and Materials Transactions A*, 2008. **39**(8): p. 1985-1992.
- [8]. Y. C. Chen, et al., Interface microstructure study of friction stir lap joint of AC4C cast aluminium alloy and zinc-coated steel. *Materials Chemistry and Physics* 2008. **111**(2-3): p. 375-380
- [9]. K. Kimpapong and T. Watanabe, Lap joint of A5083 aluminum alloy and SS400 steel by friction stir welding. *Materials Transactions*, 2005. **46**(4): p. 835-841
- [10]. M. Movahedi, et al., Mechanical and microstructural characterization of Al-5083/St-12 lap joints made by friction stir welding. *Engineering Procedia*, 2011. **10**(3297-3303).
- [11] Y. C. Chen and K. Nakata, Microstructural characterization and mechanical properties in friction stir welding of aluminium and titanium dissimilar alloys. *Materials & Design*, 2009. **30**(3): p. 469-474
- [12]. Y. H. Chen, Q. Ni, and L. M. Ke, Interface characteristic of friction stir welding lap joints of Ti/Al dissimilar alloys. *Transactions of Nonferrous Metals Society of China (English Edition)*, 2012. **22**(2): p. 299-304.
- [13] J. Wilden and J. P. Bergmann, Manufacturing of titanium/aluminium and titanium/steel joints by means of diffusion welding. *Welding and Cutting*, 2004. **3**(5): p. 285-290
- [14]. A. Fuji, et al. In-situ observation of interlayer growth during post-weld heat treatment in friction-welded joint of Titanium and Aluminium. in *Proceeding of the 7th International Symposium Japan Welding Society*. 2001. Kobe, Japan.
- [15]. A. Fuji, et al., Mechanical properties of titanium-5083 aluminium alloy friction joints. *Materials Science and Technology* 1997. **13**(8): p. 673-678
- [16]. I. M. Robertson and G. B. Schaffer, Review of densification of titanium based powder systems in press and sinter processing. *Powder Metallurgy* 2010. **53**(2): p. 146-162.
- [17]. A. Fuji, et al., Interlayer growth at interfaces of Ti/Al-1%Mn, Ti/Al-4.6%Mg and Ti/Pure Al friction weld joints by post-weld heat treatment. *Science and Technology of Welding & Joining*, 2004. **9**(6): p. 507-512.
- [18] W. V. Vaidya, et al., Improving interfacial properties of a laser beam welded Dissimilar joint of aluminium AA6056 and titanium Ti6Al4V for aeronautical applications. *Journal of Materials Science*, 2010. **45** (22): p. 6242-6245.
- [19]. S. Chen, et al., Improving interfacial reaction nonhomogeneity during laser welding-brazing aluminum to titanium. *Materials & Design*, 2011: p. Article in press.
- [20] K. Kimpapong and T. Watanabe, *Effect of welding process parameters on mechanical property of FSW lap joint between aluminum alloy and steel*. *Materials Transactions*, 2005. **46**(10): p. 2211-2217
- [21]. Y. C. Chen and K. Nakata, Microstructural characterization and mechanical properties in friction stir welding of aluminium and titanium dissimilar alloys. *Materials & Design*, 2009. **30**(3): p. 469-474